Acta Chemica Scandinavica, 1996: 50: 875–884
Printed in UK – all rights reserved

Copyright © Acta Chemica Scandinavica 1996

ACTA
CHEMICA SCANDINAVICA
ISSN 0904–213X

Structural and Conformational Properties of 1,2-Diphosphinoethane as Studied by Microwave Spectroscopy and *Ab Initio* Calculations

K.-M. Marstokk and Harald Møllendal*

Department of Chemistry, The University of Oslo, PO Box 1033 Blindern, N-0315 Oslo, Norway

Marstokk, K.-M. and Møllendal, H., 1996. Structural and Conformational Properties of 1,2-Diphosphinoethane as Studied by Microwave Spectroscopy and *Ab Initio* Calculations. – Acta Chem. Scand. 50: 875-884. ©Acta Chemica Scandinavica 1996.

The microwave spectrum of 1,2-diphosphinoethane has been investigated in the 11.0–38.0 GHz spectral region at about −40 °C. The gas phase consists of a complex equilibrium mixture of several rotameric forms of the molecule. Four conformers, two P–C–C–P *anti* and two P–C–C–P *gauche* with different orientations of the phosphino groups, have been assigned. *Anti II* was found to be the most stable conformer that possesses a dipole moment different from zero. *Anti II* is 3.4(5) kJ mol^{-1} more stable than *Gauche V*, 3.5(5) kJ mol^{-1} more stable than *Anti III*, and 4.7(6) kJ mol^{-1} more stable than *Gauche IV*.

One of these rotamers, *Anti II*, displays tunnelling in the ground vibrational state. The tunnelling frequency is 8.387(48) MHz. Tunnelling is absent in the first excited state of the C–C torsion.

The microwave work has been assisted by *ab initio* computations at the MP2/6–31G** level of theory. Computations were carried out for the 10 rotamers, six P–C–C–P *gauche*, and four *anti* forms, that are minima on the potential energy surface. These calculations predict that the four *anti* forms are all slightly more stable than any one of the six *gauche* conformers. The most stable conformation is calculated to be *Anti IV*, but this rotamer has no dipole moment for symmetry reasons, and hence cannot be observed by microwave spectroscopy. The agreement between the MP2/6–31G** predictions of rotational constants and energy differences are very good in all cases where experimental data are available.

The tendency to prefer P–C–C–P *anti* conformations is in accord with the general *gauche effect*. Intramolecular repulsion may be of importance in at least some of the *gauche* conformations, leading to a stabilisation of *anti* rotamers by repulsive forces as well.

It is well known that phosphines are excellent ligands for transition metals, and their complexes have been widely investigated.[1] Some of them are also especially effective homogenous catalysts in many chemical processes.[2] 1,2-Diphosphines, $R_1R_2PCH_2CH_2PR_3R_4$, are known to form bidentate complexes in which P–C–C–P chain of atoms take the *gauche* conformation. In addition, complexes where this chain is *anti* are also known.[1]

The simplest phosphines are volatile, poisonous, pyrophoric and possess unpleasant odours. This is presumably one reason why no structural or conformational studies have been reported for 1,2-diphosphinoethane, $H_2PCH_2CH_2PH_2$, in the gas phase in spite of the fact that this is the prototype molecule for the P–C–C–P linkage. The lack of information of the structural and conformational properties of this central compound was the major reason for carrying out the present research.

The title compound presents a complicated conformational problem because rotational isomerism is possible around the two C–P bonds and the C–C bond, with the result that as many as 10 different all-staggered conformations may exist as stable minima on the potential energy surface. These 10 forms are depicted in Figs. 1 and 2. In Fig. 1, the six rotamers having a P–C–C–P *gauche* arrangement are shown, while the four conformations having the said atoms in the *anti* position are drawn in Fig. 2. Relatively small energy differences between several of these rotamers were expected because in the isoelectronic compounds $HSCH_2CH_2SH$[3] and $ClCH_2CH_2Cl$[4] there are small energy differences between heavy-atom *gauche* and *anti* forms. Moreover, in the closely related compound $CH_3CH_2PH_2$ *gauche* and *anti*[5] with respect to the orientation of the phosphino group

* To whom correspondence should be addressed.
E-mail:harald.mollendal@kjemi.uio.no

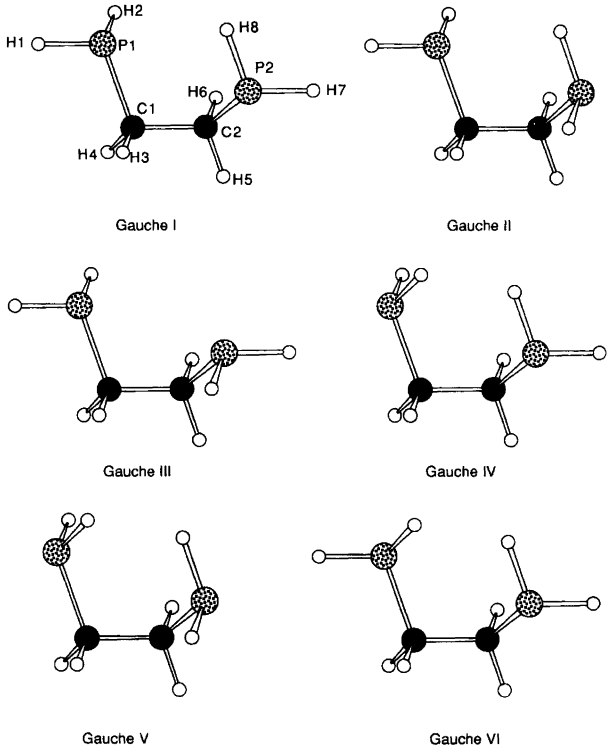

Fig. 1. The six all-staggered 'stable' conformations of 1,2-diphosphinoethane possessing a P–C–C–P *gauche* conformation. Atom numbering is shown on the *Gauche I* rotamer. *Gauche V* and *Gauche IV* were assigned in this work together with *Anti II* and *Anti III* shown in Fig. 2. *Anti II* is 3.4(5) kJ mol^{-1}more stable than *Gauche V*, 3.5(5) kJ mol^{-1} more stable than *Anti III* and 4.7(6) kJ mol^{-1} more stable than *Gauche IV*.

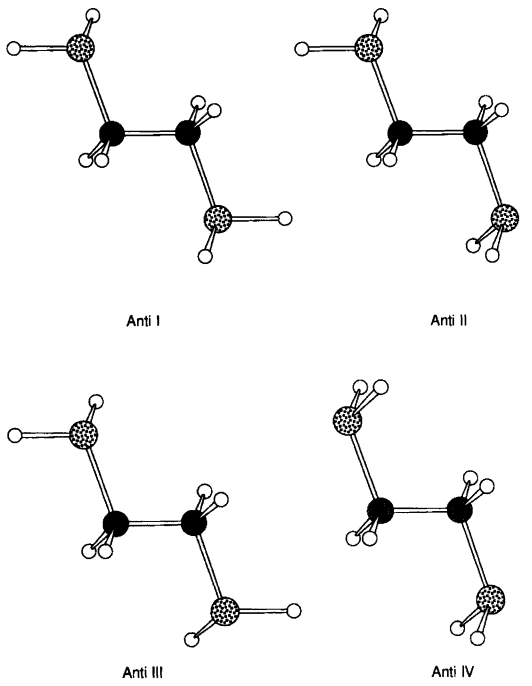

Fig. 2. The four 'stable' conformations of 1,2-diphosphinoethane having a P–C–C–P *anti* conformation.

exist with a small energy difference of 2.4(12) kJ mol^{-1}.[5a] Our expectation that 1,2-diphosphinoethane would consist of a complex mixture of several conformers in the gas phase turned out to be correct, as shown below.

Microwave (MW) spectroscopy is ideal for investigating complicated conformational equilibria where several conformers are present because of its high selectivity and specificity, and this was another motivation to investigate 1,2-diphosphinoethane by this method. Moreover, relatively high-level *ab initio* computations are often found to be useful in predicting rotational constants, dipole moments and energy differences that are sufficiently close to the experimental ones to be really helpful starting points in the spectral analysis. In addition, such computations may give important hints about rotamers that for whatever reason have not been assigned by MW spectroscopy. Such computations are thus also of interest in their own right.

Experimental

The sample utilized in this work was purchased from Strem Chemicals, Inc. The compound was purified by distillation before taking the MW spectra. The sample was kept at dry-ice temperature (−78 °C) or in a refrigerator (−40 °C) when not in use. The MW spectrum was studied using the Oslo spectrometer which is described in Ref. 6. The 11–38 GHz spectral region was investigated with the microwave absorption cell cooled to about −40 °C. Lower temperatures, which would have increased the MW spectral intensities, could not be employed owing to insufficient vapour pressure of the compound. The pressure was about 2–8 Pa when the spectra were recorded and stored electronically using the computer programs written by Waal.[7] The accuracy of the spectral measurements is presumed to be better than ±0.10 MHz and the maximum resolution to be about 0.2 MHz at a pressure of ca. 2 Pa.

Results and discussion

Ab initio *calculations*. The Gaussian 92 program package[8] running on the IBM RS6000 cluster in Oslo was employed in all the *ab initio* calculations of the conformational and structural properties of the title molecule. The 6–31G** basis set provided with the program was selected for the computations which were made using the 'frozen-core' computational procedure.[8] Electron correlation was included using the second-order Møller–Plesset (MP2) perturbation theory.[9] The geometries of all ten forms shown in Figs. 1 and 2 were fully optimized. All these conformations were found to be minima ('stable') on the potential energy surface, as no imaginary vibrational frequencies[10] were computed for any of them. Important results of the computations are summarized in Table 1 for the six P–C–C–P *gauche*, and in Table 2 for the Four *anti* rotamers. Atom numbering is shown in Fig. 1. The energy differences between the most stable

Table 1. Structure, rotational constants and dipole moments of the six stable *gauche* rotamers of $H_2PCH_2CH_2PH_2$ calculated at the MP2/6–31G** (frozen core) level.

Conformer:[a]	*Gauche I*	*Gauche II*	*Gauche III*	*Gauche IV*	*Gauche V*	*Gauche VI*
Distance/pm						
P1–H1	140.8	140.8	140.9	141.0	140.9	140.8
C1–P1	186.8	186.9	187.2	186.3	186.2	186.8
P1–H2	40.9	141.0	140.9	140.8	140.7	140.8
C1–H3	109.2	109.2	109.2	109.2	109.2	109.0
C1–H4	109.0	109.1	109.0	109.2	109.3	109.2
C1–C2	153.0	153.1	153.0	152.9	153.1	153.0
C2–H5	109.2	109.2	109.0	109.3	109.3	109.2
C2–H6	109.1	109.3	109.2	109.0	109.2	109.0
C2–P2	187.1	186.5	187.2	186.9	186.2	186.8
P2–H7	140.9	140.6	140.9	140.8	140.7	140.8
P2–H8	140.6	140.9	140.9	140.7	140.9	140.8
Angle/°						
H1–P1–C1	97.4	96.9	96.6	97.1	96.9	98.2
H1–P1–H2	95.0	94.8	94.8	94.8	94.7	94.6
P1–C1–H3	107.2	107.5	107.1	106.7	107.2	111.4
P1–C1–H4	110.8	110.2	110.6	106.0	105.1	106.2
P1–C1–C2	112.2	112.7	113.4	117.9	118.7	112.6
C1–C2–H5	108.7	109.1	108.9	108.8	109.0	108.9
C1–C2–H6	110.3	110.3	109.5	110.2	110.2	110.2
C1–C2–P2	113.1	118.3	113.4	113.3	118.7	112.6
C2–P2–H7	96.4	98.3	96.5	96.5	98.7	96.9
C2–P2–H8	99.0	96.7	96.6	99.0	96.9	98.2
Dihedral angle[b]/°						
H2–P1–C1–H3	−167.3	−165.6	−174.9	70.5	75.8	−53.0
H1–P1–C1–H3	−71.3	−70.0	−79.3	166.3	171.7	42.7
H1–P1–C1–H4	45.6	46.5	37.0	−80.8	−76.0	159.2
H1–P1–C1–C2	168.4	169.0	159.8	41.9	46.2	−81.7
P1–C1–C2–H5	182.4	190.3	179.7	184.7	195.0	187.3
P1–C1–C2–H6	−60.7	−54.1	−63.5	−58.3	−49.3	−55.2
P1–C1–C2–P2	65.0	69.8	56.1	67.4	74.8	69.9
C1–C2–P2–H7	178.8	−48.0	64.1	175.4	−49.7	−177.4
C1–C2–P2–H8	−85.4	47.9	159.7	−88.8	46.2	−81.7
Non-bonded distances [c,d]/pm						
P1···H7	464.2	300.0	385.9	482.0	324.5	465.1
P1···H8	321.7	392.8	471.1	345.8	406.2	319.7
P1···P2	350.2	368.1	342.4	365.4	386.7	356.2
Rotational constants[c]/MHz						
A	8482.7	8912.5	8234.8	8629.1	9263.3	8568.8
B	2125.9	1992.3	2176.9	2054.3	1894.1	2111.2
C	1840.4	1767.7	1865.8	1789.0	1700.3	1826.6
Principal-axes dipole moment components[e]/10^{-30} C m						
μ_a	1.40	3.37	0.00	2.33	0.00	0.00
μ_b	5.87	5.34	7.87	3.60	2.80	4.10
μ_c	3.24	1.17	0.00	3.80	0.00	0.00

[a] See Fig. 1 for definition. [b] Measured from syn = 0°. Positive dihedral angle corresponds to clockwise rotation. [c] Calculated from the structure given in this table. [d] Sum of van der Waals radii: [12] H···P = 310 pm; P···P 380 pm. [e] 1 D = 3.335 64 × 10^{-30} C m.

rotamer, *Anti IV*, and the other forms are listed in Table 3.

These tables reveal some interesting predictions: The bond distances are all very similar to the accurate r_s-values determined for *gauche* and *anti* ethylphosphine.[5b] This is also the case for the bond angles.

The variation of one bond angle, viz. the C–C–P angle, with the orientation of the phosphino group deserves comments. If the phosphino group is oriented such that the presumed direction of the lone electron pair of this group is *anti* to the C–C bond, a *large* C–C–P angle is predicted. If the lone pair is *gauche* to this bond the C–C–P angle is typically computed to be 5–6° smaller. A similar variation was also seen in the r_s-structure determined for ethylphosphine[5b] as well as in the three conformers found for 3-phosphinopropionitrile ($H_2PCH_2CH_2C{\equiv}N$).[11] This tendency has been ascribed to non-bonded repulsion between the H atoms of the phosphino group and the H atoms of the methyl or methylene groups in ethylphosphine.[5]

It is seen in Table 3 that the energies of all ten rotamers fall within a relatively narrow range of about

Table 2. Structure, rotational constants and dipole moments of the four stable *anti* rotamers of $H_2PCH_2CH_2PH_2$ calculated at the MP2/6–31G** (frozen core) level.

Conformer:[a]	*Anti I*	*Anti II*	*Anti III*	*Anti IV*
Distance/pm				
P1–H1	140.9	140.9	140.9	140.9
C1–P1	186.7	186.9	186.7	186.5
P1–H2	140.9	140.9	140.9	140.9
C1–H3	109.2	109.1	109.2	109.2
C1–H4	109.0	109.0	109.0	109.2
C1–C2	152.8	152.6	152.8	152.4
C2–H5	109.2	109.3	109.0	109.2
C2–H6	109.0	109.2	109.2	109.2
C2–P2	186.7	186.3	186.7	186.5
P2–H7	140.9	140.9	140.9	140.9
P2–H8	140.9	140.9	140.9	140.9
Angle/°				
H1–P1–C1	97.8	97.8	97.8	97.0
H1–P1–H2	94.9	94.8	94.8	94.6
P1–C1–H3	107.2	107.4	107.4	106.9
P1–C1–H4	111.5	111.5	111.2	106.9
P1–C1–C2	110.7	111.0	110.8	116.2
C1–C2–H5	109.8	110.2	110.2	110.1
C1–C2–H6	110.3	110.3	109.8	110.1
C1–C2–P2	110.7	116.1	110.7	116.2
C2–P2–H7	97.8	96.9	97.1	97.0
C2–P2–H8	96.9	97.0	97.8	97.0
Dihedral angle[b]/°				
H2–P1–C1–H3	−168.2	−168.2	−167.4	75.7
H1–P1–C1–H3	−72.3	−72.4	−71.5	171.2
H1–P1–C1–H4	44.9	44.8	45.6	−75.7
H1–P1–C1–C2	168.1	167.9	168.6	47.7
P1–C1–C2–H5	−61.9	−61.2	−61.3	−58.3
P1–C1–C2–H6	56.1	55.5	56.7	58.3
P1–C1–C2–P2	180.0	177.3	175.2	180.0
C1–C2–P2–H7	191.9	−47.9	72.8	−47.8
C1–C2–P2–H8	−72.2	47.6	168.6	47.7
Rotational constants[c]/MHz				
A	21064.4	21003.6	21073.2	20941.0
B	1424.4	1407.2	1423.6	1391.6
C	1382.4	1368.9	1382.0	1356.6
Principal-axes dipole moment components[d]/10^{-30} C m				
μ_a	0.00	1.20	0.00	0.00
μ_b	0.00	3.40	0.00	0.00
μ_c	0.00	2.30	4.10	0.00

[a–d] Comments as for Table 1.

Table 3. Energy differences relative to *Anti IV* obtained in the MP2/6-31G** (frozen core) computations.

Conformer	Relative energy/kJ mol^{-1}
Anti IV	0.0
Anti II	2.8
Anti I	4.9
Anti III	5.0
Gauche V	6.8
Gauche IV	7.1
Gauche VI	8.1
Gauche II	8.5
Gauche I	8.6
Gauche III	11.9

The total energy of *Anti IV* is −2001 546.74 kJ mol^{-1} (−762.348 858 8 hartree).

12 kJ mol^{-1}. The *anti* orientation of the P–C–C–P chain of atoms is slightly preferred, as the four *anti* forms are each computed to be more stable than any one of the six *gauche* rotamers, with *Anti IV* as the most stable one of *all* rotamers.

The orientation of the phosphino group also seems to be important for the *relative* energies of the conformers. In *Gauche V both* phosphino groups have their lone pairs *anti* to the C–C bond. This rotamer is computed to be the most stable one of the *gauche* forms (Table 3). The situation for the *anti* rotamers parallels this: here, the *Anti IV*, which also has this *anti* arrangement for both lone electron pairs, is the most stable one. These predictions are reminiscent of experimental findings made for ethylphosphine, where the rotamer having the lone pair *anti* to the C–C bond is more stable by 2.4(12) kJ mol^{-1}.[5a] In 3-phosphinopropionitrile the same conformational preference of the phosphino group was observed both for the one P–C–C–C *gauche* and the two *anti* conformers assigned in this case.[11] It is likely that the propensity for preferring an *anti* orientation of the lone electron pair of the phosphino group is a general one.

Attractive forces such as intramolecular hydrogen (H) bonding which seem to stabilize the *gauche* form of $H_2PCH_2CH_2C{\equiv}N$, making this form the most stable one,[11] appear to be of little importance in the case of the title molecule in these MP2/6–31G** computations. This effect might to a small extent be present in two of the six *gauche* conformations, i.e. *Gauche I* and *Gauche II*, both of which could have weak P–H···P hydrogen bonds, since the non-bonded H···P distances are calculated to be 322 and 300 pm, respectively (Table 1), approximately the same as the sum of the van der Waals distances of phosphorus and hydrogen (310 pm).[12] However, *Gauche I* and *Gauche II* are each calculated to be more than 8 kJ mol^{-1} less stable than *Anti IV* (Table 3). This behaviour of $H_2PCH_2CH_2PH_2$ is strikingly different from that of its amino congener, $H_2NCH_2CH_2NH_2$, where conformations similar to *Gauche I* and *Gauche II* are the most stable ones and undoubtedly stabilized by weak internal N–H···N hydrogen bonds.[13]

MW spectrum and assignment of the ground vibrational state of Anti II. 1,2-Diphosphinoethane has a very rich spectrum with absorptions occurring every few MHz throughout the entire MW range. A striking feature of this spectrum in the 20–38 GHz range is a series of strong lines protruding from the dense background of weaker ones. The peak absorption intensities of the strongest members of this series, which are the strongest ones in the whole spectrum, are roughly 4×10^{-7} cm^{-1} at −40 °C. Moreover, all these lines were noted to be split by 0.5–0.6 MHz into two components of equal intensity. This splitting is presumed to be caused by large-amplitude tunnelling, as described in the next paragraph.

The *ab initio* calculations above indicate that *Anti IV*

is the most stable form of 1,2-diphosphinoethane (Table 3). However, this rotamer has *zero* dipole moment (Table 2) for symmetry reasons, and therefore cannot be observed by MW spectroscopy. The rotamer with the second lowest energy is predicted to be *Anti II*. This conformer is computed to be 2.8 kJ mol^{-1} less stable than *Anti IV* (Table 3), and it was therefore decided to search for this rotamer first.

The rotational constants in Table 2 indicate that *Anti II* is an almost prolate symmetrical top with the asymmetry parameter $\kappa \approx -0.99$. Its largest dipole moment component is calculated (Table 2) to lie along the *b*-inertial axis. The MW spectrum was thus predicted to possess a strong series of high-*J* *b*-type $K_{-1}=1\leftarrow 0$ *Q*-branch transitions in the 20–38 GHz range. Attempts to fit the series of strong, split lines just mentioned taking their average frequencies, met with immediate success. All ^bQ-transitions up to $J=38$ were soon assigned. Some selected transitions are shown in Table 4.*

The assignments of low- and intermediate-*J* *b*-type *R*-branch transitions were made after some searching. Some of these transitions turned out to be split, while others were broad, or displayed no resolvable splitting. In no cases were splittings larger than about 2 MHz observed for any of these transitions.

Anti II is computed to have a significant dipole moment component along the *c*-axis (Table 2). The two $K_{-1}=1\leftarrow 0$ and $K_{-1}=2\leftarrow 1$ ^cQ-branch series occurring in the investigated spectral range were predicted to be the strongest *c*-type lines belonging to the spectrum of this rotamer. The former of these two series was assigned first in the 11–15 GHz region, where they are among the strongest transitions encountered here. All these *c*-type *Q*-branch transitions display splittings much larger (typically about 17 MHz; see examples in Table 4) than the *b*-type transitions.

The strongest members of the latter $K_{-1}=2\leftarrow 1$ series were then easily assigned in the 30–38 GHz spectral region. These transitions are split by 14–15 MHz. It was noted that they are much less intense than the ^bQ-lines occurring here. This is an indication that the dipole moment component along the *c*-inertial axis (μ_c) is considerably less than μ_b, in keeping with the predictions for *Anti II* (Table 2). The $K_{-1}=2\leftarrow 1$ series could be followed up to a maximum value of $J=72$. The splittings become progressively a bit smaller as *J* increases. A few ^cR-type lines were also assigned. They are split in the same manner as the ^cQ-branch lines are.

The frequencies of the *a*-type *R*-branch transitions were predicted next. Individual ^aR-lines could not be assigned with certainty presumably owing to their low intensities. This is in agreement with the small value of μ_a predicted for *Anti II* (Table 2). However, the ^aR-pile-ups of the high-K_{-1} members were easily observed at frequencies predicted using the spectroscopic constants in Table 5 for the $J=7\leftarrow 6$ up through the $J=13\leftarrow 12$ transitions. None of these pile-ups are split by several MHz, such as *c*-type transitions are. The splitting of the *a*-type lines are definitely small and presumably of the same magnitude as those seen for the *b*-type transitions (2 MHz).

Tunnelling. Our explanation for the doublet splittings seen for the *b*- and *c*-type lines (Table 5) is that they arise from

Table 4. Selected transitions from the MW spectrum of the ground vibrational state of *Anti II* of 1,2-diphosphinoethane.

Transition $J'_{K_{-1},K_{+1}}\leftarrow J''_{K''_{-1},K''_{+1}}$		Observed frequency[a]/MHz	Obs.−calc. freq./MHz
b-type			
$8_{1,7}\leftarrow 8_{0,8}$	(+)←(+)	20047.00	0.06
	(−)←(−)	20047.53	−0.03
$12_{1,11}\leftarrow 12_{0,12}$	(+)←(+)	20894.45	−0.04
	(−)←(−)	20895.01	−0.05
$17_{1,16}\leftarrow 17_{0,17}$	(+)←(+)	22470.19	−0.09
	(−)←(−)	22470.75	−0.03
$21_{1,20}\leftarrow 21_{0,21}$	(+)←(+)	24191.74	−0.14
	(−)←(−)	24192.32	−0.01
$19_{0,19}\leftarrow 18_{1,18}$	(+)←(+)	36528.02	−0.27
	(−)←(−)	36528.52	0.20
$25_{1,24}\leftarrow 25_{0,25}$	(+)←(+)	26374.17	−0.14
	(−)←(−)	26374.73	0.01
$28_{1,27}\leftarrow 27_{2,26}$	(+)←(+)	27498.91	0.13
	(−)←(−)	27500.31	0.03
$31_{1,30}\leftarrow 31_{0,31}$	(+)←(+)	30623.39	−0.08
	(−)←(−)	30623.99	0.09
$33_{1,32}\leftarrow 33_{0,33}$	(+)←(+)	32324.36	0.04
	(−)←(−)	32324.96	0.19
$36_{1,36}\leftarrow 35_{2,33}$	(+)←(+)	25161.06	−0.20
	(−)←(−)	25162.61	0.23
$37_{1,36}\leftarrow 37_{0,37}$	(+)←(+)	36182.52	−0.01
	(−)←(−)	36183.13	0.02
$41_{1,41}\leftarrow 40_{2,38}$	(+)←(+)	32712.51	−0.17
	(−)←(−)	32714.34	0.02
c-type			
$15_{1,15}\leftarrow 15_{0,15}$	(−)←(+)	17132.51	−0.17
	(+)←(−)	17115.22	−0.02
$19_{0,19}\leftarrow 18_{1,17}$	(−)←(+)	29921.77	−0.29
	(+)←(−)	29904.32	0.04
$19_{1,19}\leftarrow 19_{0,19}$	(−)←(+)	15936.39	0.14
	(+)←(−)	15918.82	−0.17
$24_{1,24}\leftarrow 24_{0,24}$	(−)←(+)	14199.01	0.22
	(+)←(−)	14181.59	0.04
$28_{1,28}\leftarrow 28_{0,28}$	(−)←(+)	12684.51	0.06
	(+)←(−)	12667.32	0.14
$32_{1,32}\leftarrow 32_{0,32}$	(−)←(+)	11126.09	0.04
	(+)←(−)	11108.91	0.12
$47_{2,46}\leftarrow 47_{1,46}$	(−)←(+)	37714.95	−0.08
	(+)←(−)	37700.14	−0.13
$53_{2,52}\leftarrow 53_{1,52}$	(−)←(+)	32959.12	0.02
	(+)←(−)	32944.68	0.00
$59_{2,58}\leftarrow 59_{1,58}$	(−)←(+)	28090.46	0.14
	(+)←(−)	28076.01	−0.08
$64_{2,63}\leftarrow 64_{1,63}$	(−)←(+)	24085.68	0.00
	(+)←(−)	24071.75	0.18
$71_{2,70}\leftarrow 71_{1,70}$	(−)←(+)	18791.16	−0.04
	(+)←(−)	18777.46	0.02

[a] ±0.10 MHz.

* The full spectra of the four conformers assigned in this work are available from the authors upon request, or from the Molecular Spectra Data Center, National Institute of Standards and Technology, Molecular Physics Division, Bldg. 221, Rm. B265, Gaithersburg, MD 20899, USA, where they have been deposited.

Table 5. Spectroscopic constants[a,b] of the (+)- and (−)-states of *Anti II* of 1,2-diphosphinoethane.

No. of transitions:	169	
R.m.s. dev.[c]/MHz:	0.088	
	(+)-state	(−)state
A_v/MHz	20731.289(32)	20731.945(31)
B_v/MHz	1409.968 8(15)	1409.970 8(15)
C_v/MHz	1371.259 8(15)	1371.259 1(15)
Δ_J/kHz	0.147 18(70)	0.146 58(70)
Δ_{JK}/kHz	−2.012(33)	−0.737(32)
Δ_K/kHz	[d]	[d]
δ_J/kHz	0.005 924(27)	0.005 865(29)
δ_K/kHz	[d]	[d]
Δ^e/MHz	8.387(48)	

[a] As defined by Nielsen.[14] [b] Uncertainties represent one standard deviation. [c] Root-mean-square deviation. [d] Pre-set at zero in least-squares fit.

a large-amplitude motion of one of the phosphino groups. A 120° rotation around the C1–P1 bond (Fig. 2) produces a conformation that is spectroscopically identical to one depicted in this figure. The ground state is a symmetrical or (+) state, while the first excited state of this double minimum potential is an antisymmetrical or (−) state. The separation between these states, Δ, is about half the splitting observed for the *c*-type transitions with the smallest values of *J* (ca. 8.5 MHz).

The tunnelling motion results in different selection rules. An operation that interchanges the conformation of the phosphino group is presumed to invert the spatial direction of the *c*-axis dipole moment component, while no such inversion occurs for the other two dipole moment components. The selection rules are thus those of a rigid rotor plus (−)←(+), or (+)←(−) for the *c*-type transitions, while the *a*- and *b*-type transitions obey rigid-rotor plus (+)←(+) or (−)←(−)selection rules. The *c*-type lines should thus be split into two components roughly equal to the rigid-rotor frequency plus or minus ca. 8.5 MHz, while the *a*- and *b*-type transitions should be unsplit by tunnelling. The small splittings (<ca. 2 MHz) observed for several of the *b*-type lines are caused by effects comparable to the ordinary vibration–rotation coupling that separates excited states from the ground vibrational state.

In order to derive the spectroscopic constants for this tunnelling the computer program ASMIXX written by Nielsen[14] was utilized. This program employs an effective two-level rotation–vibration Hamiltonian including quartic and sextic centrifugal distortion constants and coupling terms of the μ- or *L*-type.[14,15] The reduced Hamiltonian has the following definition:[14]

$$H_{red} = |0\rangle\{H_r^{(0)} + H_d^{(0)}\}\langle 0| + |1\rangle\{H_r^{(1)} + H_d^{(1)} + W_{01}\} \times \langle 1| + |0\rangle H_c \langle 1| + |1\rangle H_c \langle 0|$$

$$H_r^{(v)} = X^{(v)}J_x^2 + Y^{(v)}J_y^2 + Z^{(v)}J_z^2$$

$$H_d^{(v)} = \{\text{Watson quartic and sextic centrifugal distortion}\}^{(v)}$$

$$W_{01} = \langle 1|H_{vib}^{\circ}|1\rangle - \langle 0|H_{vib}^{\circ}|0\rangle$$

$$H_c = \mu_{yz}(J_yJ_z + J_xJ_y) \text{ or } L_xJ_x$$

A total of roughly 280 transitions were assigned for the ground vibrational state of *Anti II*. 169 of these were used to derive the spectroscopic constants shown in Table 5. The transitions selected for this purpose were all well resolved. In the least-squares procedure used to derive the parameters of this table, the rotational constants, and three of the quartic centrifugal distortion constants of both the (+)- and the (−)-states were fitted together with the separation between the (+)- and the (−)-state, $\Delta = W_{01}$. The use of only three quartic centrifugal distortion constants is warranted because *Anti II* is almost a symmetrical rotor. No significant values for μ- or *L*-type coupling terms could be determined. Attempts to include sextic centrifugal distortion constants yielded no improvement. Our model yields a good fit to the observed frequencies, as shown in Table 4, as the root-mean-square deviation of 0.128 MHz is comparable to the experimental uncertainty of 0.10 MHz.

Inspection of Table 5 reveals that there is a small, but significant difference between the *A* rotational constants of the (+)- and (−) states of 0.656 MHz, and insignificant differences between the *B* and the *C* rotational constants of the two states. A rather large difference is seen for the Δ_{JK} Watson[16] centrifugal distortion constant of the two states whereas the Δ_J and δ_J centrifugal distortion constants are quite similar for the (+)- and (−)-state.

1,2-Diphosphinoethane is not the first example of a phosphine exhibiting tunnelling. This effect has also been observed for *gauche*-ethylphosphine, where the tunnelling frequency is about 5 MHz.[5]

Attempts to determine the dipole moment by Stark effect measurements failed because the low-*J* transitions were so weak that quantitative measurements could not be made. This was also the case for the three other rotamers assigned in this work.

Vibrationally excited states. The ground-state spectrum was accompanied by satellite spectra that could be ascribed to vibrationally excited states of *Anti II*. Two excited states of what is presumed to be successively excited states of the torsional vibration around the C–C bond were assigned; their spectroscopic constants (*A*-reduction I^r-representation[16]) are found in Table 6.

84 *b*- and *c*-type transitions as well as ^aR-branch pile-ups were assigned for the first excited state of the C–C torsion. *No* doublet splittings owing to tunnelling were observed for both the *b*- and the *c*-type lines of the first excited C–C torsional state. This behaviour contrasts that observed for the ground vibrational state, where small splittings were often observed for the *b*-type, and larger splittings (13–17 MHz) were always seen for the *c*-type lines (previous paragraph). Any hypothetical splitting must be less 0.2 MHz, the resolution in this experiment, if such splittings exist at all. The reason why tunnelling splittings are absent is perhaps that the double-

Table 6. Spectroscopic constants[a,b] of excited states of the torsion around the C–C bond of *Anti II* of 1,2-diphosphinoethane.

Vibrational state:	$v_T=1$[c]	$v_T=2$[d]
No. of transitions:	84	39
R.m.s. dev.[e]/MHz:	0.068	0.074
A_v/MHz	20 248.080(12)	19 817.181(40)
B_v/MHz	1411.857 6(12)	1413.784 5(35)
C_v/MHz	1374.426 8(12)	1377.627 7(38)
Δ_J/kHz	0.153 82(93)	0.75(12)
Δ_{JK}/kHz	−1.310 1(94)	−1.42(55)
Δ_K/kHz	[f]	[f]
δ_J/kHz	0.005 480 3(91)	0.004 97(10)
δ_K/kHz	[f]	[f]

[a] *A*-reduction, I^r-representation.[18] [b] Uncertainties represent one standard deviation.[c] This excited state is *not* split by tunnelling; see text. [d] This excited state seems to be split by tunnelling; see text.[e] Root-mean-square deviation. [f] Pre-set at zero in least-squares fit.

minimum symmetry of the wavefunction is lost in the first excited C–C torsional state.

Relative intensity measurements using selected transitions performed largely as described in Ref. 17 yielded a frequency of 118(22) cm^{-1} for this vibration, compared to 99 cm^{-1} found in the *ab initio* computations above (not given in Table 2).

39 *b*-type transitions and [a]*R*-branch pile-ups were assigned for the second excited state of the torsion. A fairly constant small splitting of ca. 0.28 MHz was resolved for the strongest members of the $K_{-1}=1\leftarrow0$ [b]*Q* series. It was not possible to resolve splittings for the weaker *b*-type transitions apparently because it is so small. The average frequencies of the split lines were used together with transitions for which the splitting could not be resolved to determine the spectroscopic constants shown in Table 6.

It is noted that the splitting seen for this excited state is typically about half of what was observed for the ground vibrational state. This points to considerable coupling between torsion and tunnelling. No *c*-type lines were assigned with certainty, presumably because they are very weak and split by several MHz, rendering their assignments not obvious in this dense spectrum. It is assumed that these lines would have been assigned provided they had been unsplit, because in such a case they would have been twice as intense, and their frequencies would have been very accurately predicted from the *b*-type transitions. The reason why the transitions of the second excited C–C torsional state apparently are split in the same manner as the ground-state lines are split, perhaps means that symmetry of the wavefunction is now the same as it is in the ground vibrational state.

Only the [a]*R*-pile-ups were observed for the third excited state of the C–C torsional vibration, yielding $B+C\approx2796.8$ MHz. The changes of the rotational constants upon excitation (Tables 5 and 6) are fairly constant for this mode. This is typical for a fairly harmonic vibration.[18]

[a]*R*-pile-ups of two further excited states were assigned. The values of $B+C$ are ≈2778.3 and ≈2778.9 MHz, respectively. The intensities of each of these are roughly 25% of the intensities of the ground-state pile-up, corresponding to a frequency of roughly 220 cm^{-1}. It was not possible to find *b*- and *c*-type lines belonging to these two excited states. The second lowest vibration is computed (not included in Table 2) to have a frequency of 167 cm^{-1}, and the third lowest normal mode is calculated to have a frequency of 197 cm^{-1}. The two approximate values of $B+C$ of 2778.3 and 2778.9 MHz, respectively, found for the pile-ups may belong to the first excited state of these two normal mode, but it is not possible to say which $B+C$ belong to the first excited state of which normal vibration.

Assignment of Anti III. *Anti I* and *Anti III* have approximately the same energy according to the MP2/6–31G** results given in Table 3. *Anti I* has no dipole moment for symmetry reasons (Fig. 2 and Table 2), and will therefore not have a MW spectrum. However, *Anti III* has only a *c*-type spectrum for symmetry reasons. This rotamer is computed to be 2.2 kJ less stable than *Anti II* (Tables 3 and 7). The assignment of the comparatively strong [c]*Q* $K_{-1}=1\leftarrow0$ series was first made in the 11–17 GHz spectral region. The [c]*Q* $K_{-1}=2\leftarrow1$, which extends throughout the whole MW region, was then found with ease and followed up to $J=78$. [c]*R*-type lines were searched for next and found after some trials. A total of 54 *c*-type transitions were assigned and used to determine the rotational constants shown in Table 8. None of the *c*-type lines was split (to within the resolution of ca. 0.2 MHz).

Inversion or rotation of the two phosphino groups should invert the spatial direction of the *c*-dipole moment in this case (Fig. 2) and lead to a tunnelling spectrum similar to the one described above for *Anti II*. The fact that no splitting is seen for *Anti III* perhaps indicates that the barrier is higher here than in the case of *Anti II*. The fact that both phosphino groups must be involved in the tunnelling process in *Anti III*, whereas only one group can be involved in the case of *Anti II*, would also tend to reduce possible splitting.

A search for *a*- and *b*-type lines was made, but none

Table 7. Experimental and MP2/6–31G** energy differences[a] relative to the energy of *Anti II*.

	Energy difference/kJ mol^{-1}	
	Experimental[b]	MP2/6-31G**
$E_{Gauche\ V}-E_{Anti\ II}$	3.4(5)	4.0
$E_{Anti\ III}-E_{Anti\ II}$	3.5(5)	2.2
$E_{Gauche\ IV}-E_{Anti\ II}$	4.7(6)	4.3

[a] Taken from Table 3. [b] Uncertainties represent one standard deviation.

Table 8. Spectroscopic constants[a,b] of the ground state of *Anti III* of 1,2-diphosphinoethane.

No. of transitions:	54
R.m.s. dev.[c]/MHz:	0.074
A_0/MHz	20778.234(29)
B_0/MHz	1427.185 4(39)
C_0/MHz	1385.593 0(39)
Δ_J/kHz	0.171 3(54)
Δ_{JK}/kHz	−1.400(31)
Δ_K/kHz	[d]
δ_J/kHz	0.006 908(16)
δ_K/kHz	[d]

[a,b] Comments as for Table 6.[c,d] Comments as for [e,f] in Table 6.

of them was found, presumably because these two dipole moment components are zero for symmetry reasons in accord with the symmetry of *Anti III*. The fact that only *c*-type spectra have been observed is one indication that *Anti III* has indeed been assigned, and that this rotamer has not been confused with a vibrationally excited state of *Anti II*, because these two conformers are predicted to have rather similar rotational constants, but quite different dipole moment components (Table 2).

The first excited state of the C–C torsion whose calculated frequency is 95 cm^{-1} (not given in Table 2), was searched for, but not identified; the reason is believed to be weakness and high spectral density.

Assignment of Gauche V. This rotamer is computed to be 4.0 kJ mol^{-1} (Tables 3 and 7) less stable than *Anti II* and the most stable *gauche* conformer. It is predicted to have only a *b*-axis dipole moment component that is different from zero for symmetry reasons (Fig. 1 and Table 1). Searches for the ^bQ-lines predicted to be the strongest ones for this rotamer were successful after many trials. The ^bR-branch transitions were found next after many trial lines had been tested in least-squares fits. The spectroscopic constants obtained from 46 *b*-type transitions with a maximum value of $J=35$ (for the $35_{4,31} \leftarrow 35_{3,32}$ transition) are given in Table 9. Vibrationally excited states, especially the first excited C–C torsional state (calculated frequency 93 cm^{-1}; not included in Table 1) were searched for, but not found, presumably because they are weak.

No *a*- or *c*-type lines were found as expected although their hypothetical frequencies could be very accurately predicted from the constants listed in Table 9. This is one indication that *Gauche V* has indeed been identified. Other evidence that *Gauche V* has been correctly assigned and not confused with any one of the other five *gauche* conformations such as, e.g. *Gauche III* and *Gauche VI* (both of which are also predicted to have only a *b*-dipole moment component that is different from zero for symmetry reasons), is the fact that the rotational constants computed for *Gauche V* are much closer to the experimental rotational constants in Table 9, than the rotational constants calculated for *Gauche III* and *Gauche VI*, respectively, as seen in Table 1. In addition, the two last-mentioned forms are computed to have somewhat higher energies than that of *Gauche V* (Table 3).

Assignment of Gauche IV. This rotamer is calculated to have an energy close to that of *Gauche V* (Table 3). This conformer was searched for next. 122 transitions of the *b*- and *c*- variety were ultimately assigned for *Gauche IV*, whose spectroscopic constants are reported in Table 10. No *a*-type lines were identified with certainty, presumably because they are too weak to be identified in this dense spectrum. This is in accord with the prediction of Table 1 that μ_a is the smallest dipole moment component of this conformer. The maximum value of J was 63 for the $63_{8,56} \leftarrow 63_{7,56}$ transition. The normal Watson quartic and one sextic[16] centrifugal distortion constant, Φ_{JK}, had to be used (Table 10) in order to get a satisfactory least-squares fit.

The orientation of the phosphino groups of *Gauche IV* is similar to those of *Anti II* (one having the lone pair of phosphorus *anti* to the C–C bond, and one *gauche*, respectively; Figs. 1 and 2) where tunnelling was a predominant spectral feature. However, no tunnelling was observed for *Gauche IV*. It is possible that the reason for this is a higher barrier to tunnelling in this case than in the case of *Anti II*.

It can be seen in Table 1 that *Gauche I* and *Gauche II*

Table 9. Spectroscopic constants[a,b] of the ground state of *Gauche V* of 1,2-diphosphinoethane.

No. of transitions:	46
R.m.s. dev.[c]/MHz:	0.074
A_0/MHz	9244.292(19)
B_0/MHz	1904.980 3(88)
C_0/MHz	1709.118 2(86)
Δ_J/kHz	0.763(49)
Δ_{JK}/kHz	−8.743(57)
Δ_K/kHz	60.7(22)
δ_J/kHz	0.206 72(71)
δ_K/kHz	2.31(11)

[a,b] Comments as for Table 6. [c] Comments as for [e] in Table 6.

Table 10. Spectroscopic constants[a,b] of the ground state of *Gauche IV* of 1,2-diphosphinoethane.

No. of transitions:	122
R.m.s. dev.[c]/MHz:	0.074
A_0/MHz	8596.864 3(41)
B_0/MHz	2071.659 3(16)
C_0/MHz	1802.283 8(16)
Δ_J/kHz	1.440 3(21)
Δ_{JK}/kHz	−11.834(10)
Δ_K/kHz	46.06(19)
δ_J/kHz	0.355 18(19)
δ_K/kHz	3.525(19)
Φ_{JK}/Hz	0.102 5(12)

[a–c] Comments as for Table 8.

also have substantial components of the dipole moment along the *b*- and *c*-axis just as *Gauche IV*. Yet, the rotational constants predicted for the two first-mentioned conformations (Table 1) are in considerably worse agreement with those in Table 10 than the 'theoretical' rotational constants calculated for *Gauche IV* in Table 1. The relative intensities of the *b*- and *c*-type lines assigned in this case agree well with those calculated from the dipole moment components predicted for *Gauche IV* in the same table. Moreover, the MP2/6–31G** predictions in Table 3 that the energies of *Gauche I* and *Gauche II* are somewhat higher that those of *Gauche IV* are additional evidence that *Gauche IV* has indeed been assigned and not confused with any other *gauche* rotamer.

No vibrationally excited states were assigned, although they were searched for. This failure is again ascribed to spectral weakness.

MW search for further conformations. The above assignments include all the strongest transitions seen in the MW spectrum as well as many weak lines and transitions of intermediate intensity. However, several hundred unassigned, mostly weak lines remain unaccounted for in the 11–38 GHz spectral region. A large number of these transitions undoubtedly belong to unassigned vibrationally excited states of the four rotamers whose assignments are described above. Unidentified impurities may also be a possibility.

Numerous unsuccessful attempts were made to assign these unidentified transitions to each of the four *gauche* forms that had not been assigned. The starting points in these searches were the rotational constants and dipole moment components given in Table 1. The fact that each of these conformations is predicted to possess sizable dipole moments as well as the observation that no strong unassigned lines remain, is evidence that additional unassigned *gauche* forms must have relatively high energies compared to the energy of *Anti II*. Our estimate is then that the energy difference between any one of the four unassigned *gauche* rotamers and the most stable conformer assigned here, *Anti II*, must be larger than 3 kJ mol^{-1}. This estimate is considered to be conservative.

Energy differences. The energy differences between the four conformers assigned in this investigation were made by relative intensity measurements observing the precautions of Ref. 17. The MP2/6–31G** dipole moment components in Tables 1 and 2 were used, because experimental dipole moments are not available.

It was found that *Anti II* is the most stable one of the *assigned* conformers. Whether it is more stable than the completely unpolar *Anti IV* rotamer, which is predicted in the MP2/6–31G** computations to be the most stable form of the molecule, is impossible to say. *Anti II* is found to be 3.4(5) kJ mol^{-1} more stable than *Gauche V*, 3.5(5) kJ mol^{-1} more stable than *Anti III*, and 4.7(6) kJ mol^{-1} more stable than *Gauche IV*. The liberal uncertainties given here represent one standard deviation. They have been estimated by taking the experimental as well as the uncertainties of the calculated dipole moments into account.

The present findings are compared with the theoretical predictions in Table 7. The agreement is very satisfactory.

Structure. It is seen from Tables 5 and 8–10 that the experimental rotational constants of all four assigned rotamers are close to those calculated from the MP2/6–31G** structure in Tables 1 and 2. In fact, the agreement is better than about 1.5% for all three rotational constants in all four cases. This is as good an agreement as one can expect because the *ab initio* structure is an approximation of the equilibrium structure, while the rotational constants in Tables 5 and 8–10 reflect the r_0-structures. Moreover, the structural parameters for these four conformers are all very similar to their experimental counterparts in the closely related molecule ethylphosphine,[5b] as remarked above. No experimental data are at hand that could really improve the MP2/6–31G** (frozen core) structures. The structures shown in Tables 1 and 2 are therefore adopted as *plausible* structures for *Gauche IV, Gauche V, Anti II* and *Anti III*. It is expected that any full experimental structure that might be determined in the future for these four rotamers will be close to the ones shown in these two tables.

Conclusions

This study has demonstrated that 1,2-diphosphinoethane consists of a complex equilibrium mixture of at least four rotameric forms in the gas phase. Both P–C–C–P *anti* and *gauche* forms contribute to the equilibrium and the energy differences between them are not great.

The conformational properties of $H_2PCH_2CH_2PH_2$ are strikingly different from those of its amino analogue, $H_2NCH_2CH_2NH_2$. The latter compound has two N–C–C–N *gauche* conformations each stabilized by weak internal H bonds as its most stable conformers[13] while the corresponding two P–C–C–P *gauche* rotamers are definitely high-energy forms of 1,2-diphosphinoethane, if they are stable at all.

There are probably several reasons why these two congeners exhibit varied conformational properties. One important factor is that nitrogen is considerably more electronegative than phosphorus. The so-called *gauche effect*[19] predicts that the tendency to prefer a X–C–C–X *gauche* atomic arrangement *increases* with the electronegativity of the substituent X. The finding that the heavy-atom *gauche* forms of 1,2-diaminoethane are relatively more stable than the *gauche* forms of 1,2-diphosphinoethane is in agreement with this effect.

Moreover, conditions for forming intramolecular H bonds are not good, or perhaps completely absent, in *Gauche I* and *Gauche II* of $H_2PCH_2CH_2PH_2$, because the geometries of the H bonds are unfavourable

(Table 1), the low electronegativity of phosphorus, and the low polarity of the P–H bond. The H bonding situation in the corresponding two conformers of $H_2NCH_2CH_2NH_2$ are much more favourable.[13]

The existence of repulsive forces between the two amino groups in $H_2NCH_2CH_2NH_2$ and between the phosphino groups in $H_2PCH_2CH_2PH_2$ are quite probable in some of the heavy-atom *gauche* forms of the two compounds. These forces are offset by internal H bonding and the *gauche* effect in the former molecule, but likely to predominate slightly in the latter. The conformational properties of 1,2-diphoshpinoethane thus resembles more its isoelectronic congeners $HSCH_2CH_2SH$[3] and ClCH2CH2Cl,[4] which both prefer *anti* conformer(s),[3d,4] than its homologue $H_2NCH_2CH_2NH_2$.

Acknowledgement. Mrs. Anne Horn is thanked for drawing the figures. This work has received support from The Research Council of Norway (Programme for Supercomputing) through a grant of computer time.

References

1. Corbridge, D. E. C. *Phosphorus. An Outline of its Chemistry, Biochemistry and Technology,* Elsevier, Amsterdam 1978.
2. (a) Shaw, B. L. In: Aleya, E. C. and Meek, D. W., Eds., *Catalytic Aspects of Metal Phosphine Complexes, Advances in Chemistry Series* Vol. 196, Am. Chem. Soc., Washington, DC 1982, p. 101; (b) Pignolet, L. H., Ed., *Homogenous Catalysis with Metal Phosphine Complexes,* Plenum Press, New York 1983.
3. (a) Schultz, G. and Hargittai, I. *Acta Chim. Acad. Sci. Hung. 75* (1973) 381; (b) Hargittai, I. and Schultz, G. *J. Chem. Phys. 84* (1986) 5220; (c) Nandi, R. N., Su, C. F. and Harmony, M. D. *J. Chem. Phys. 81* (1984) 1051; (d) Bultinck, P., Goeminne, A. and Van de Vondel, D. *J. Mol. Struct. (Theochem) 334* (1995) 101.
4. (a) Kveseth, K. *Acta Chem. Scand. Ser. A 28* (1974) 482; (b) Kveseth, K. *Acta Chem. Scand., Ser. A 29* (1975) 307.
5. (a) Durig, J. R. and Cox, A. W. *J. Chem. Phys. 64* (1976) 1930; (b) Groner, P., Johnson, R. D. and Durig, J. R. *J. Chem. Phys. 88* (1988) 3456.
6. Guirgis, G. A., Marstokk, K.-M. and Møllendal, H. *Acta Chem. Scand. 45* (1991) 482.
7. Waal. Ø. Personal communication 1994.
8. Frisch, M., Trucks, G. W, Head-Gordon, M., Gill, P. M. W., Wong, M. W., Foresman, J. B., Johnson, B. G., Schlegel, H. B., Robb, M. A., Replogle, E. S., Gomperts, R., Andres, J. L., Raghavachari, K., Binkley, J. S., Gonzalez, C., Martin, R. L., Fox, D. J., Defrees, D. J., Baker, J., Stewart, J. J. P. and Pople, J. A., *Gaussian 92,* Revision C, Gaussian, Inc., Pittsburgh, PA 1992.
9. Møller, C. and Plesset, M. S. *Phys. Rev. 46* (1934) 618.
10. Hehre, W. J., Radom, L., Schleyer, P. v. R. and Pople, J. A. *Ab Initio Molecular Orbital Theory,* Wiley, New York 1985, p. 227.
11. Marstokk, K.-M. and Møllendal, H. *Acta Chem. Scand., Ser. A 37* (1983) 755.
12. Pauling, L. *The Nature of the Chemical Bond,* 3rd Ed., Cornell University Press, New York 1960, p. 260.
13. (a) Marstokk, K.-M. and Møllendal, H. *J. Mol. Struct. 49* (1978) 221; (b) Kazerouni, M. R., Hedberg, L. and Hedberg, K. *J. Am. Chem. Soc. 116* (1994) 5279; (c) Bultnick, P., Goeminne, A. and Van de Vondel, D. *J. Mol. Struct. (Theochem) 339* (1995) 1.
14. Nielsen, C. J. *Acta Chem. Scand., Ser. A 31* (1977) 791.
15. Harris, D. O., Harrington, H. W., Luntz, A. C. and Gwinn, W. D. *J. Chem. Phys. 44* (1966) 3467.
16. Watson, J. K. G. In: Durig, J. R., Ed., *Vibrational Spectra and Structure,* Elsevier, Amsterdam 1977, Vol. 6., p 1.
17. Esbitt, A. S. and Wilson, E. B. *Rev. Sci. Instrum. 34* (1963) 901.
18. Herschbach, D. R. and Laurie, V. W. *J. Chem. Phys. 37* (1962) 1668.
19. Wolfe, S. *Acc. Chem. Res. 5* (1972) 102.

Received January 4, 1996